October 2002

ELSEVIER

Materials Letters 56 (2002) 454–459

MATERIALS LETTERS

www.elsevier.com/locate/matlet

Impedance spectroscopy of tetragonal zirconia polycrystals doped with ceria

E.N.S. Muccillo *, D.M. Ávila

Centro Multidisciplinar para o Desenvolvimento de Materiais Cerâmicos, CCTM-Instituto de Pesquisas Energéticas e Nucleares, C.P. 11049, Pinheiros, Sao Paulo, S.P., 05422-970, Brazil

Received 5 May 2001; accepted 1 June 2001

Abstract

Tetragonal zirconia polycrystals doped with x mol% ceria ($8 \le x \le 20$) have been prepared by mechanical mixing using alumina as milling media. Impedance spectroscopy has been used to verify the effect produced by alumina on grain and grain boundary resistivities. For comparison purposes, more homogeneous specimens have been prepared by the coprecipitation technique. The main results show that impedance spectra exhibit predominantly ionic character for $x \ge 12$ in the temperature range of measurements. Alumina impurity has a minor effect on electrical resistivity whereas the blocking of charge carriers at grain boundaries is found to be primarily dependent on the grain size.

PACS: 81.20.E; 84.37; 81.40
Keywords: Ce-TZP; Microstructure; Impedance spectroscopy; Solid electrolytes; Zirconia

1. Introduction

Ce- and Y-doped tetragonal zirconia polycrystals (Ce-TZP and Y-TZP, respectively) have been extensively studied due to their improved thermomechanical properties compared with other zirconia-based ceramics [1]. These studies have shown as a common feature that the sintering and densification of most commercially available powders involve an intergranular silica-rich glassy phase at the sintering temperature. This intergranular glassy phase has a large impact on the tetragonal to monoclinic transformation and on mechanical properties of Ce-TZP and Y-TZP ceramics [2,3]. For Y-stabilized zirconia it, was shown [4] that this intergranular phase can be at least partially removed from the grain boundaries with small additions of alumina. The confinement of this glassy phase at triple junctions by alumina, known as "scavenger effect," has also been observed in Ce-TZP [5]. This effect has been shown to increase slightly both the mechanical strength and fracture toughness in ceria-12 mol% zirconia specimens containing a suitable amount of alumina [5].

Concerning electrical properties, ceria-doped zirconia is considered to be a mixed conductor unlike most stabilized zirconia systems. In the whole range of solid solution, however, the electrical properties of this system vary considerably. Recent works in this system have shown that pure electronic conduction is observed

* Corresponding author. Fax: +55-11-3816-9343.
E-mail address: enavarro@net.ipen.br (E.N.S. Muccillo).

0167-577X/02/$ - see front matter © 2002 Elsevier Science B.V. All rights reserved.
PII: S0167-577X(02)00527-X

for ceria-rich solid solutions [6], whereas in the low-ceria (up to 20 mol% CeO_2) concentration range, the electrical resistivity is independent on the oxygen partial pressure [7]. In addition, the activation energy is about 1 eV, a value usually found in most zirconia-based ionic conductors. It was suggested [8] that the observed scatter in the resistivity results obtained by different authors in the past could be explained if silicon impurity effects had be taken into account.

In this study, ZrO_2: x mol% CeO_2 ($8 \le x \le 20$) were prepared by the powder mixing technique to verify the effect of dopant concentration and aluminum impurity on the electrical resistivity measured by impedance spectroscopy. For comparison purposes, specimens with a more homogeneous microstructure have also been prepared by the coprecipitation technique.

2. Experimental

ZrO_2 (99.6%, DK-1 type, Zirconia Sales), CeO_2 (>99%, IPEN), $ZrOCl_2 \cdot 8H_2O$ (>99%, BDH) and $Ce(NO_3)_3 \cdot 6H_2O$ (>99.5%, IPEN) were used as starting materials for solid solution preparations by the powder mixing and coprecipitation techniques, respectively. ZrO_2: x mol% CeO_2 solid solutions with $x = 8$, 10, 12, 15 and 20 were prepared by the powder mixing technique. The required amounts of ZrO_2 and CeO_2 were mechanically mixed (Turbula, T2C) in ethanol for 6 h using alumina as milling media. This procedure resulted in a deliberately contamination with alumina and other minor impurities. Cylindrical specimens of 12-mm diameter and 1–2-mm thickness were prepared by uniaxial pressing followed by cold isostatic pressing at 206 MPa. Sintering was carried out at 1500 °C for 1 h.

Specimens with a nominal concentration of 12 mol% CeO_2 have been prepared by the coprecipitation technique. A full description of this process can be found in Ref. [9]. Pressing of the calcined powders into pellets was carried out in a similar way as for mixed powder specimens. Sintering was performed at 1500 °C for 2 h.

Cerium contents in sintered specimens have been determined by thermal neutron activation analysis. Alumina contamination in sintered specimens was evaluated by inductively coupled plasma emission spectroscopy.

Crystallographic measurements have been carried out to determine the crystal structure, phase content and theoretical density. Measurements were performed with Rigaku Geigerflex or Philips X'Pert MPD diffractometers. The theoretical density was obtained from the unit cell weight and volume. The relative volume (V) fractions of monoclinic (m) and tetragonal (t) or cubic (c) phases in the as-sintered specimens were evaluated by the corresponding intensities of the main diffraction peaks of each phase.

Values of green density (d_g) have been calculated by measuring sample dimensions and weight. Apparent sintered density (d_s) values have been determined by the immersion technique.

Fractured surfaces were observed in a Philips XL30 scanning electron microscope. Grain size distributions were evaluated on polished and thermally etched surfaces.

Electrical resistance was measured on sintered specimens by impedance spectroscopy technique using an HP 4192A impedance analyzer. The measurements were conducted over a frequency range of 5 Hz to 13 MHz over a temperature range from 300 to 600 °C in air. Platinum paste (Demetron A308) was used to form electrode contacts on the parallel surfaces of the specimens.

Results were analyzed in the impedance mode using a special computer program [10]. The grain and grain boundary resistance (R) values were used to calculate the corresponding intragrain and intergrain resistivities (ρ). The temperature dependence of the electrical resistivity is expressed using the Arrhenius equation. To take into account the difference in the grain boundary density of sintered specimens a correction based on the determined average grain size (G) was done according to [11]. The blocking of charge carriers at grain boundaries was evaluated by calculating the blocking factor, α_R [12].

3. Results and discussion

The actual concentration of ceria in the sintered specimens is shown in Table 1. The calculated and nominal values agree reasonably well, indicating that there was no significant loss of dopant during processing.

Table 1
Nominal, measured and calculated concentrations of dopant in specimens prepared by the powder mixing technique

Specimen	Nominal (mol% CeO_2)	Measured (mol% Ce)	Calculated (mol% CeO_2)
MP08	8	8.00 ± 0.10	7.24 ± 0.09
MP10	10	10.40 ± 0.20	9.49 ± 0.20
MP12	12	12.88 ± 0.20	11.86 ± 0.20
MP15	15	15.50 ± 0.40	14.41 ± 0.40
MP20	20	20.60 ± 0.80	19.52 ± 0.80

The expected contamination with alumina from the milling media reached a value of 0.7 wt.% determined by inductively coupled plasma emission spectroscopy.

Fig. 1 shows the diffraction patterns in the 2θ range from 20° to 40° for sintered pellets. The main reflections of the monoclinic and tetragonal/cubic phases can be easily identified. Moreover, in the whole patterns no peaks were found that could be assigned to spurious phases like isolated cerium or aluminum oxide.

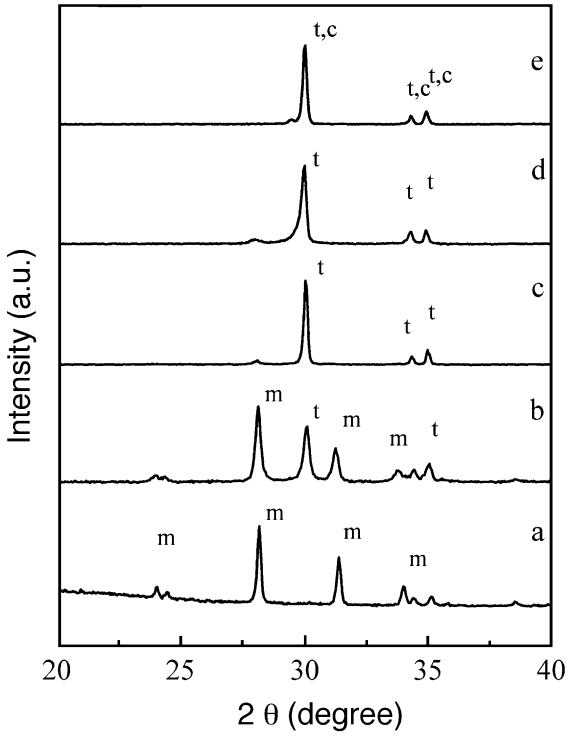

Fig. 1. X-ray diffraction patterns of sintered specimens prepared by the powder mixing technique.

Table 2
Values of tetragonal phase volume fraction (V_t), and relative green (percent d_g) and sintered (percent d_s) densities

Specimen	V_t (%)	Percent d_g	Percent d_s
MP08	12	53	92.3
MP10	58	53	92.3
MP12	~ 100	54	92.2
MP15	100	54	92.1
MP20	100[a]	55	92.0
CP12	100	37	98.0

[a] Tetragonal + cubic phases.

From the patterns shown in Fig. 1, the relative fraction of tetragonal phase for each specimen was calculated. As can be seen in Table 2 for ceria concentrations of 12 mol% or higher, there is a complete stabilization of the tetragonal phase. For the 20 mol% specimen, a small fraction of cubic

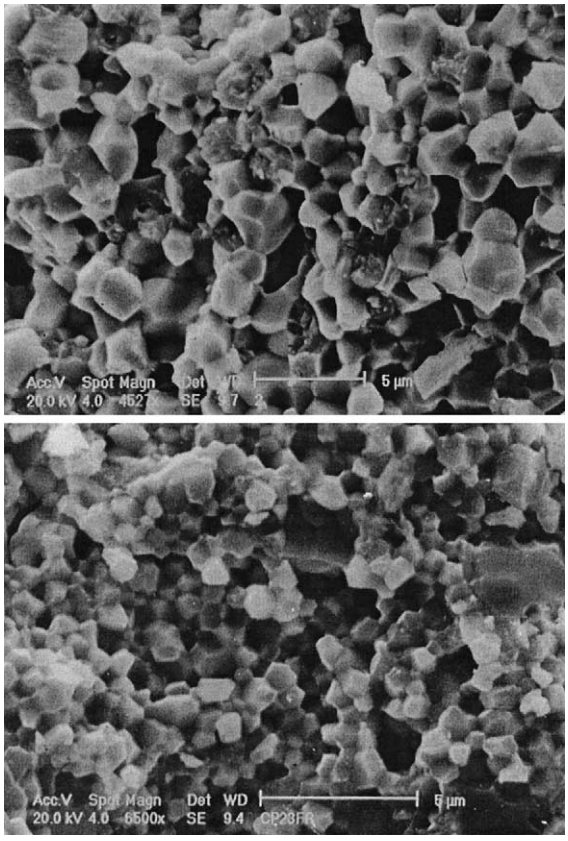

Fig. 2. Scanning electron microscopy micrographs of fracture surfaces of specimens prepared by powder mixing (top) and coprecipitation (bottom) techniques.

phase is expected from phase diagram considerations [13]. Specimens prepared with coprecipitated powders (CP12) are fully stabilized.

The relative green and sintered densities are also shown in Table 2. The relative green density values are comparatively higher for specimens prepared by powder mixing due to better particle packing. Sintered density values are consistent with the inherent difficulty to densify zirconia–ceria solid solutions. For the coprecipitated specimen, an improvement on synthesis processing has been achieved [9], allowing for attainment of high sintered density.

Fig. 2 shows scanning electron micrographs of fractured surfaces of specimens prepared by the powder mixing (top) and coprecipitation (bottom) techniques. For the coprecipitated specimen, the calculated average grain size was 500 nm. For other specimens, the grain size distributions were quite irregular and only an approximate value around 2 μm could be estimated.

Impedance diagrams detected on sintered specimens at 500 °C are shown in Fig. 3. In the temperature range of measurements, all diagrams show the same features: a predominant high-frequency semicircle and a smaller low-frequency semicircle. The high-frequency semicircle describes the intragrain resistance and capacitance relaxation. The low-frequency semicircle is related to the conductivity blocking effects at grain boundaries or intergrain resistivity. For all specimens except the MP10 one, part of a third semicircle, assigned to the electrode response, is detected. The existence of the electrode semicircle suggests that the conductivity is essentially ionic in these temperature and composition ranges. In contrast, for the MP10 sample no electrode semicircle was observed in the entire temperature range of measurements. From this result, it is reasonable to expect an important contribution of electronic conduction for solid solutions with ceria concentrations lower than 12 mol%. The specimen containing the lower Ce concentration, MP08, is quite resistive and could not be accurately measured.

A typical impedance diagram at 490 °C obtained for a specimen prepared with coprecipitated powders is shown in the insert of Fig. 3. The main observed difference relative to the impedance spectra of other specimens is the relative contributions of intra- and intergrain resistivities. In this case, the blocking of charge carriers at grain boundaries is the most important contribution to the total electrolyte resistivity.

Fig. 4 shows Arrhenius plots of the intragrain resistivity for all studied specimens. The resistivity does not vary significantly with composition, but there is a net tendency to increase with increasing ceria concentration. For the specimen prepared with

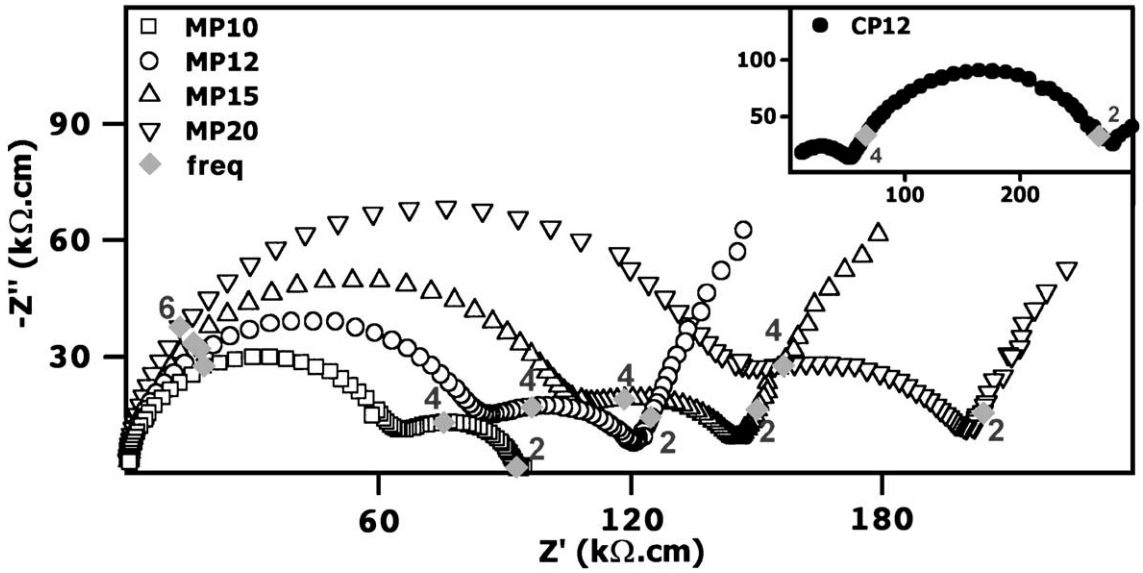

Fig. 3. Impedance spectra of sintered zirconia–ceria ceramics.

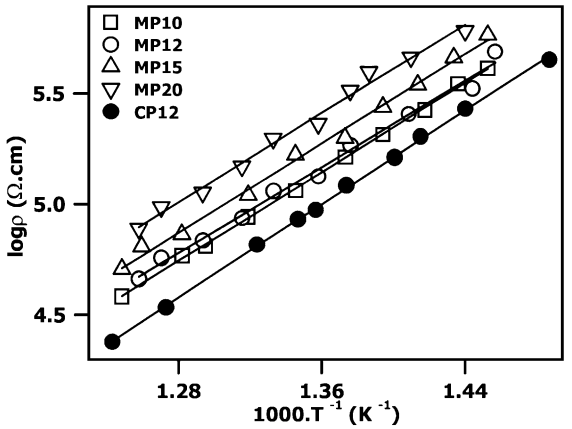

Fig. 4. Intragrain resistivity for sintered zirconia–ceria ceramics.

the coprecipitated powder, the intragrain resistivity is slightly lower probably due to a better chemical homogeneity of the individual grains.

The Arrhenius plots for the intergrain resistivity of specimens prepared by the powder mixing technique show the same trend as that for the intragrain resistivity. Fig. 5a shows intergrain plots for specimens with different silica content and grain sizes, but similar ceria concentration. The intergrain resistivity of specimens prepared with coprecipitated powders is almost one order of magnitude higher than that of specimens prepared by the powder mixing technique. This means that the blocking of charge carriers at grain boundaries is considerably higher in specimens prepared with coprecipitated powders, as shown in Fig. 5b. As expected, the blocking factor, α_R, decreases steadily with increasing temperature, but is >100% larger than that of specimens prepared by the powder mixing technique. Specimens prepared with coprecipitated powder have a high silica content because this impurity comes from the cerium nitrate precursor (Si content of 0.15 wt.%). The CeO_2 precursor has a Si content < 0.006 wt.%, and it is expected that the distribution of this impurity inside the sintered ceramic to be mostly confined at triple grain junctions due to alumina contamination during processing. However, these specimens have quite different grain sizes, and it is known that the influence of grain size on the intergrain resistivity increases with decreasing grain sizes [11]. The intergrain resistivity corrected for the grain size effect is shown in Fig. 5c for both specimens. The resistance per square centimeter of grain boundary

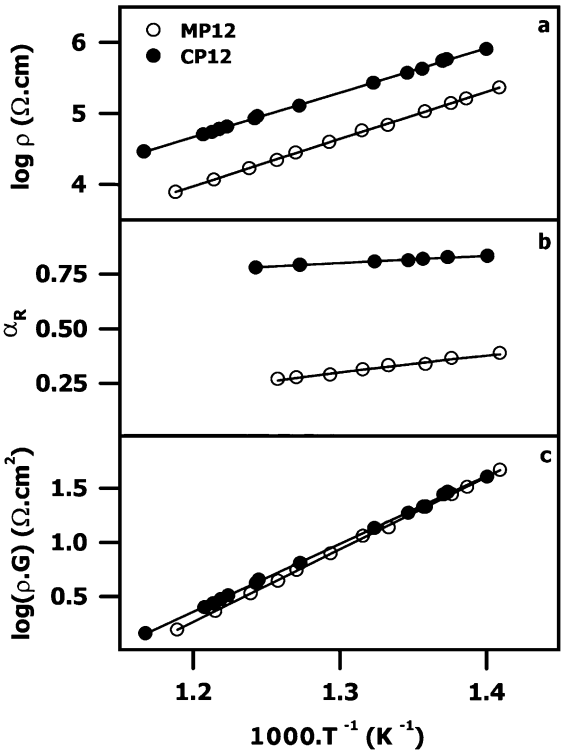

Fig. 5. Arrhenius plots for the intergrain resistivity (a); variation of blocking factor with temperature (b); and variation of specific resistance with temperature (c) for specimens prepared by the powder mixing (○) and coprecipitation techniques (●).

surface, ($\rho_{gb}G$), of both specimens does not differ significantly. This result shows that not only the silicon content, but mainly the average grain size is a determinant factor for the increased resistivity of the chemically prepared Ce-TZP ceramic.

Calculated values of thermal activation energy and pre-exponential factor for studied specimens are listed in Table 3. In all cases, the correlation factor obtained in the linear regression was better than 0.999.

Table 3
Values of activation energy (E) and pre-exponential (ρ_0) factor for intragrain (g) and intergain (cg) resistivity

Specimen	E_g (eV)	E_{gb} (eV)	ρ_{0g}	ρ_{0gb}
MP10	1.000	1.315	2.02	0.82
MP12	1.004	1.326	2.46	0.88
MP15	1.003	1.324	3.18	0.96
MP20	1.034	1.321	2.69	1.40
CP12	1.042	1.245	0.72	13.52

The activation energy values are typical of the values found in oxygen ion conductors (~ 1 eV). The intergrain activation energy values are slightly higher than those for intragrain as usual. The pre-exponential factors confirm that the low conductivity of Ce-TZP ceramics compared with Y-TZP is mainly due to low extrinsic conduction of grains.

4. Conclusions

The main results show that the intragrain resistivity in zirconia–ceria ceramics does not vary considerably with composition in the tetragonal phase field. In contrast to results observed in Y-TZP ceramics, silicon impurity plays a minor role in the intergrain resistivity. Most of the observed difference, in this case, comes from the difference in average grain size of specimens.

Acknowledgements

We would like to express our thanks to Zirconia Sales for providing the ZrO_2 sample and to CNEN, CNPq (300934/94-7), FAPESP (99/10798-0) and FINEP/PRONEX for the financial support.

References

[1] J.D. Cawley, W.E. Lee, in: R.W. Cahn, P. Haasen, E.J. Kramer (Eds.), Materials Science and Technology—a Comprehensive Treatment, in: M.V. Swain (Ed.), Structure and Properties of Ceramics, vol. 11, VCH, Weinheim, Germany, 1994, p. 47.
[2] P.E.R. Morel, I.W. Chen, J. Am. Ceram. Soc. 71 (1988) 343.
[3] M.L. Mecartney, J. Am. Ceram. Soc. 70 (1987) 54.
[4] M. Miyayama, H. Yanagida, A. Asada, Am. Ceram. Soc. Bull. 64 (1985) 660.
[5] J. Wang, C.B. Ponton, P.M. Marquis, J. Mater. Sci. Lett. 12 (1993) 702.
[6] G. Chiodelli, G. Flor, M. Scagliotti, Solid State Ionics 91 (1996) 109.
[7] R.F. Reidy, G. Simkovich, Solid State Ionics 62 (1993) 85.
[8] S. Meriani, Mater. Sci. Eng., A 109 (1989) 121.
[9] E.N.S. Muccillo, D.M. Ávila, Ceram. Int. 25 (1999) 345.
[10] M. Kleitz, J.H. Kennedy, in: P. Vashishta, J.N. Mundy, G.K. Shenoy (Eds.), Fast Ion Transport in Solids, Electrodes and Electrolytes, North-Holland, Amsterdam, 1979, p. 185.
[11] M. Miyayama, H. Inoue, H. Yanagida, J. Am. Ceram. Soc. 66 (1983) C164.
[12] M. Kleitz, H. Bernard, E. Fernandez, E. Schouler, in: A.H. Heuer, L.W. Hobbs (Eds.), Advances in Ceramics, Science and Technology of Zirconia I, vol. 3, ACS, Columbus, OH, 1981, p. 310.
[13] E. Tani, M. Yoshimura, S. Somiya, J. Am. Ceram. Soc. 66 (1983) 506.